Clarification of Phase Separation Mechanism of Sodium Borosilicate Glasses in Early Stage by Nuclear Magnetic Resonance

Tetsuo Yazawa,*,† Koji Kuraoka,† Tomoko Akai,† Norimasa Umesaki,† and Wei-Fang Du‡,§

Optical Materials Department, Osaka National Research Institute, Midorigaoka 1-8-31, Ikeda City, Osaka 563-8577, Japan, and New Energy and Industrial Technology Development Organization, Midorigaoka 1-8-31, Ikeda City, Osaka 563-8577, Japan

Received: September 24, 1999; In Final Form: December 23, 1999

Nuclear magnetic resonance (NMR) spectra have been used to investigate the spinodal phase separation of sodium borosilicate glasses in the early stage, in which the phase separation is induced by rapidly quenching as opposed to heat treatment at a constant temperature. The experimental results show that the spinodal phase separation occurs under the quenching rates of 10^6 and 10 K/s. Although the domain size of the phase separation increases with decreasing quenching rate, ^{11}B NMR spectra and ^{29}Si MAS NMR spectra do not vary with the change of the domain size of the spinodal phase separation resulting from oxygen diffusion on quenching. The structure analysis by NMR measurement indicates that the oxygen diffusion is controlled by a vacancy mechanism. On the basis of these NMR data, a structural model in the initial stage of the spinodal phase separation is proposed. The model suggests that the oxygen vacancy migrates by rotating itself to neighboring-bridged oxygen and reacting with the neighboring-bridged oxygen while the coordination number of the boron and silicon does not change. By the rotation and reaction, borons are connected together along the motion trace of the vacancy. According to the model, double-boron-group chains and triborate-group chains with high connectivity may be formed on rapidly quenched sodium borosilicate glasses.

1. Introduction

Sodium borosilicate is a typical spinodal phase separation glass and source material for porous glass, which is finding widespread application in industry.[1−3] By the spinodal phase separation, two interconnected phases, one rich in silica and the other rich in boric oxide, are thereby induced. These two phases differ in their solubility behavior: when treated with dilute acid, the boron-rich phase readily dissolves, leaving the silica-rich phase almost untouched. This results in a highly porous glass. The relation between the propagation of the spinodal phase separation under heat treatment at a constant temperature and the pore characteristics in sodium borosilicate glass has been extensively studied in previous work by a variety of techniques.[4,5] On the basis of this spinodal phase separation, the porous glasses with highly connective mesopores and macropores, which are promising materials for separation membranes, enzyme and catalyst supports, photonic materials etc.,[1,6−13] can be obtained.

The systematic theory concerning kinetics and thermodynamics of the spinodal decomposition was first proposed by Cahn et al. in the 1960s.[14−16] This theory has been developed in many studies.[17−20] The early stage of spinodal phase separation, in which the spinodal decomposition is induced by rapidly quenching rather than heat treatment at a constant temperature, was usually thought to have a close relation with diffusion in glasses,[21] whereas the later stage of spinodal phase separation, in which spinodal decomposition is induced by heat treatment at a constant temperature, is a coalescence process. In this stage, large inhomogeneity regions grow at the expense of solution of smaller ones. The dependence of the domain size r of the separated phase on heat-treated time t at a constant temperature in the later stage was investigated quantitatively by replication electron microscopy,[18−20] which was found to increase with the cube root of heat treatment time t, i.e., $r \propto t^{1/3}$, when the coalescence occurs.

Despite these efforts, however, the early stage of the spinodal decomposition, i.e., the propagation of the spinodal phase separation under a continuous cooling from the melting state, is still little explored since the theoretical study by Cahn et al. in the 1960s.[14−16] The kinetic theory of the spinodal decomposition predicts that the domain size of the spinodal decomposition is reduced greatly under high cooling rate. This suggests that it is difficult in the experimental investigation on the early stage to use ordinary techniques such as replication electron microscopy etc. Especially, experimental data on the atomic-scale details of structure change in the early stage of the spinodal phase separation are rare. There are few experimental results that give direct microscopic information on atomic-scale dynamics in the early stage of the spinodal phase separation. The lack of investigation in the rapid-quenched region prevents us from developing new porous glasses with micropores, which are thought to be promising materials as membranes with "molecular sieving" properties. From the point of view of materials design for molecular sieving etc., it is very important to study the mechanism of the spinodal phase separation in the initial stage and its relation with structure change on rapid quenching since the composition and the micropore characteristics of the porous glass are controlled precisely by a clarification of the relationship.

* Corresponding author.
† Osaka National Research Institute.
‡ New Energy and Industrial Technology Development Organization.
§ Present address: Optical Materials Department, Osaka National Research Institute, Midorigaoka 1-8-31, Ikeda City, Osaka 563-8577, Japan.

10.1021/jp993416b CCC: $19.00
Published on Web 02/10/2000

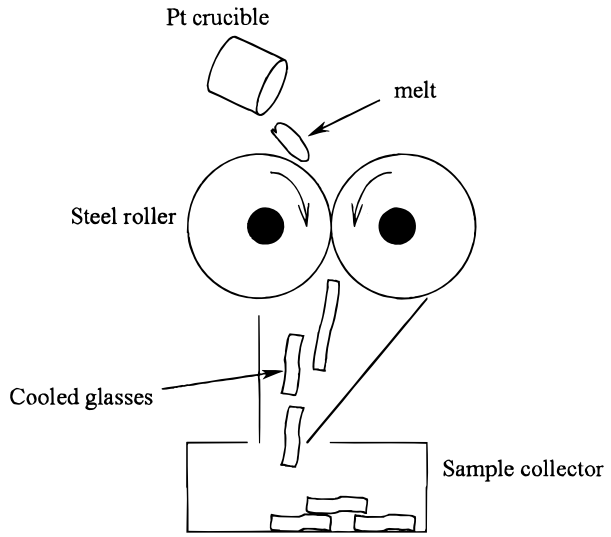

Figure 1. Schematic illustration of the roller-quenched process for sodium borosilicate glasses.

Nuclear magnetic resonance (NMR) spectroscopy has been an important tool in characterizing borate and borosilicate glass structure for several decades. It has been shown that boron atoms exist as either 3-fold or 4-fold coordination with network oxygen. In particular, the relative proportions of four- and three-coordinated boron (BO_4 vs BO_3 groups, the N_4:N_3 ratio) in the borosilicate glasses can be quantified accurately using ^{11}B NMR.[22−31] However, few NMR studies have examined the sodium borosilicate glass samples that were prepared with varying quench rates within the spinodal region. As there is no energy barrier for the spinodal decomposition and the decomposition in the early stage is controlled by diffusion processes, the structure of the spinodal decomposed glasses on quenching are expected to be quite different from those resulting from nucleation and growth. In this paper, we use ^{11}B NMR and ^{29}Si MAS NMR, together with Raman spectra, to study the atomic-scale details of structure change in the early stage of spinodal phase separation for the sodium borosilicate glass samples that were prepared with varying quench rates. In addition, the present work employed a nitrogen adsorption−desorption method to investigate the spinodal phase separation that allows the domain size of the spinodal phase separation in initial stage to be seen clearly. On the basis of the correlation between the domain size and the NMR and Raman spectra data, we describe the structural change on quenching and the mechanism of the spinodal phase separation in the initial stage.

2. Experimental Procedures

2.1. Sample Preparation. A typical glass with the composition of $9.4Na_2O-25.4B_2O_3-65.2SiO_2$ (mol %), which can exhibit the spinodal phase separation by heat treatment, was used in this investigation. The sodium borosilicate glasses were prepared from reagent grade sodium carbonate, boric acid, and silica. First, the reagent-grade chemicals were thoroughly mixed. Then the mixtures were placed in a platinum crucible and fused at 1673 K in an electric furnace for 60 min. The melts were quenched by two methods, i.e., air quench and roller quench. The air-quenched samples were prepared by pouring ∼25 g of melt into carbon molds. Such a quench rate is about ∼10 K/s. The twin-roller-quenched technique consists of melting and then dropping the specimens between a pair of rapidly rotating steel rollers that are held together under pressure, as illustrated in Figure 1. The drop solidifies while passing through the rollers.

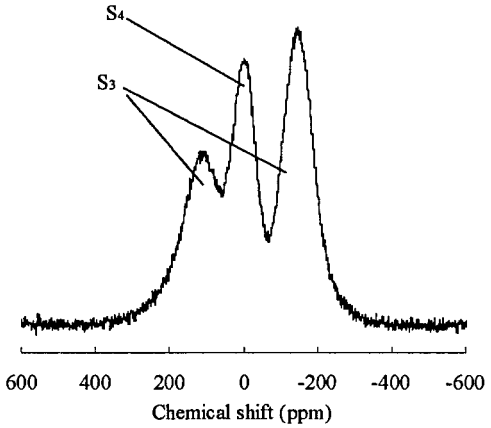

Figure 2. Pulse ^{11}B NMR spectrum of the sodium borosilicate glass sample where the adsorption curve corresponds to the resonance from 3-fold- and 4-fold-coordinated boron, respectively.

Therefore, the rapidly quenched glass in the shape of thin uniform films can be obtained. The quenching rate of glass increased with increasing rotation speed and pressure on the rollers. The theoretical calculation of the quenching rate τ of the twin-roller-quenched method is given by[32]

$$\tau = \Delta T/\Delta t \approx [(T_m - T_g)v]/d$$

where T_m and T_g are respectively the initial temperature of the melt and the glass transition temperature and Δt ($\approx v/d$) is the time duration of the contact between the melt and the rollers, where v is the linear velocity of the roller and d is the distance traveled by the melt during solidification, which is determined by rotation speed, pressure, and radius of the rollers, etc. The speed of the steel roller in the present study is ∼3000 rpm. At such a rotation speed, the roller-quenched samples are estimated to have a quench rate of $\sim 10^6$ K/s by the present twin-roller-quenched apparatus.

2.2. NMR Measurements. *(1) ^{11}B NMR Measurement.* The ^{11}B NMR experiments were performed with a Chemagnetics CMX-200 operating at 64.19 MHz by the pulse method. The spectra were obtained by Fourier transforming free-induction decay. The length of the 90° pulse was set to 4.5 μs by using H_3BO_3 solution. For the measurement, we used a pulse as short as 1 μs to avoid the undesired quadrupole effect.[33] Typically, 64 scans were used to obtain the spectra. Figure 2 shows a typical example of the ^{11}B NMR spectrum in borate glasses. The spectra S_3 and S_4 are from 3-fold- and 4-fold-coordinated boron, respectively. In general, the difference in NMR spectra between the BO_3 unit and BO_4 unit is due to the structural difference between BO_3 and BO_4. The BO_3 unit employs a planar structure in which the boron lies at the center of an oxygen triangle. This configuration produces the large electric field gradient vertical to the plane, and as a result, the nuclear quadrupole moment of ^{11}B ($I = {}^3/_2$) in BO_3 becomes considerably large (2.6−2.8 MHz).[34] Due to the large quadrupole moment, the adsorption from the central transition of ^{11}B ($-{}^1/_2 \leftrightarrow {}^1/_2$) shows a doublet pattern from the second-order quadrupole interaction, as shown in Figure 2. On the other hand, in the BO_4 unit, the boron is located at the center of an oxygen tetrahedron. The quadrupole moment becomes small because of the symmetry around ^{11}B, so that a single resonance line is observed for the ($-{}^1/_2 \leftrightarrow {}^1/_2$) transition. These two specific ^{11}B adsorptions from BO_3 and BO_4 can easily be separated, which enables one to obtain the fraction of each species. The method has been widely used to obtain the fraction of BO_3 and BO_4 in glasses since the late 1960s.[26−31]

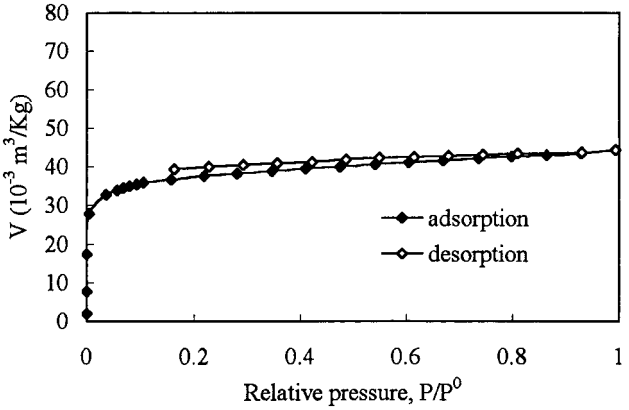

Figure 3. Adsorption isotherm curve of the roller-quenched sample after leaching.

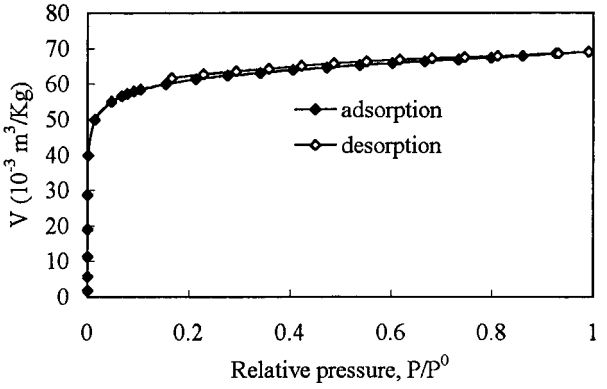

Figure 4. Adsorption isotherm curve of the air-quenched sample after leaching.

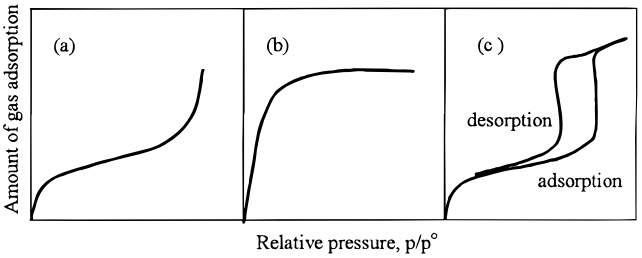

Figure 5. Essential features of the adsorption isotherm for (a) nonporous solids, (b) microporous solids, and (c) mesoporous solids

The pulse-FT NMR method employed in the recent NMR spectrometer is usually more convenient than the continuous wave method, which had been used until the 1970s. However, there is a drawback in this method. The acquisition of the signal is started immediately after the strong RF pulse, which is in the range of hundreds of watts. Since the receiver is designed to detect signals in the nanowatt range, it takes some time for the receiver to recover from the pulse. During this period, the so-called dead time, some portion of the signal is lost depending on the length of the signal in the time domain. In this case, the loss of the signal from B in BO_3 is larger than that in BO_4. This causes an error in quantitative analysis from the area of each spectrum (Figure 2). To calibrate the error, we measured a series of $x$$Na_2O-(1-x)B_2O_3$ glasses, where N_4 is well-known to be $x/(1-x)$,[22] and determined the calibration factor. We also measured $Li_2O-B_2O_3$ glasses and some sodium borate crystals and confirmed that this calibration factor can be used in a wide compositional range.[35]

(2) ^{29}Si Magic Angle Spinning (MAS) NMR Measurement. ^{29}Si MAS NMR spectra were collected under 4.7 T with 39.789 MHz. The 90° pulse was set to 4.5 μs. In the present experiment, a 30° pulse (1.5 μs) was used to reduce the repetition time. The spectrum was accumulated 3200 times with the repetition time of 8 s. The sample was spun at 3000 Hz.

2.3. Measurement of the Domain Size of Phase Separation. The pore size was measured after leaching out the boron-rich phase in samples so as to estimate the domain size of the phase separation. The glasses prepared by the above methods were etched using an aqueous solution of 3 N HNO_3 at 371 K and were washed with water and dried. The specific surface areas and the pore size distribution of the samples were determined by nitrogen adsorption (Belsorp 28, Bel Japan Inc.). Prior to the measurement, the samples were evacuated at 423 K for 3 h. The specific surface areas were calculated by the BET method,[36] and the pore size distribution was analyzed by the MP method.[37]

2.4. Raman Spectra Measurement. Unpolarized Raman spectra were obtained using the triple monochromator (Jobin-Yvon, T64000). Light scattering experiments utilized a single-model laser light of 5145 Å from an Ar-ion laser (coherent, Innova 305).

3. Results

3.1. Spinodal Phase Separation on Quenching. Figures 3 and 4 show the adsorption−desorption isotherms of the quenched samples that were leached from the boron-rich phase. According to the pore diameter within a given solid, porous materials are classified as the micropore type with the pore diameter less than 2 nm, the mesopore type with the pore diameter between 2 and 50 nm, and the macropore type with the pore diameter more than 50 nm by the International Union of Pure and Applied Chemistry.[38] These porous solids usually exhibit a different behavior of nitrogen adsorption and desorption as compared with a nonporous solid when they are exposed in a closed space to nitrogen at some definite pressure.[39−46] The essential features of the adsorption−desorption isotherm of these porous solids and nonporous solid are illustrated in Figure 5.[47] It can be seen from Figures 3 and 4 that samples clearly possess an extensive pore network of the micropore type. They are characterized by a large amount of adsorption at a low relative pressure and a plateau that is nearly horizontal, as indicated in Figure 5. The experimental results confirm that the spinodal phase separation occurs at the quenching rates of both 10^6 and 10 K/s.

TABLE 1: Measurement Results of the Surface Area and Pore Volume of the Samples Quenched at Different Cooling Rates

cooling condition	cooling rate (K/s)	pore volume (10^{-2} cm^3/g)	surface area (10^2 m^2/g)
roller-quenching	~10^6	6.60	1.409
air-quenching	~10	10.6	2.301

By comparison of Figure 3 with Figure 4, the amount of adsorbed nitrogen increases with decreasing cooling rate. This indicates that the spinodal phase separation is further propagated in the air-quenched sample. The change of the domain size of the phase separation with quenching rate can be also confirmed by the measurement of pore volume and surface area, as shown in Table 1. The measurement results show that the surface area and the pore volume increase with decreasing cooling rate. When the cooling rate decreases from 10^6 to 10 K/s, the pore volume and surface area increase from 6.60×10^{-2} cm^3/g and 1.409×10^2 m^2/g to 1.06×10^{-1} cm^3/g and 2.301×10^2 m^2/g, respectively.

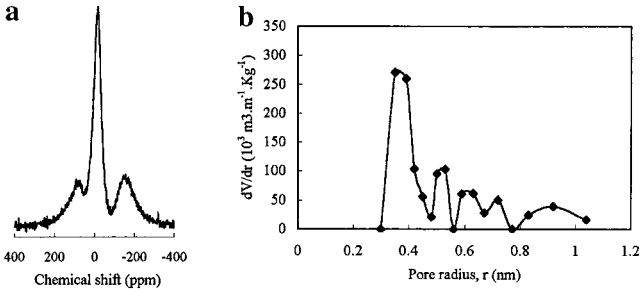

Figure 6. Correlation of the ^{11}B NMR spectrum and the phase separation in sodium borosilicate glasses by roller-quenching: (a) ^{11}B NMR spectrum of the roller-quenched sample; (b) pore size distribution of the roller-quenched sample after leaching.

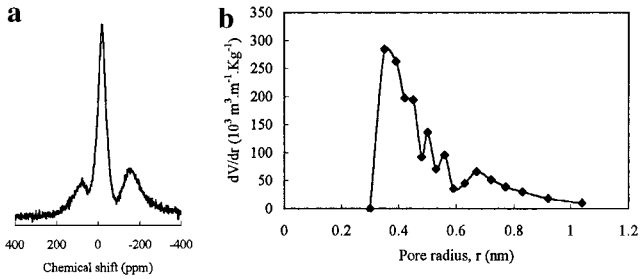

Figure 7. Correlation of the ^{11}B NMR spectrum and the phase separation in sodium borosilicate glasses by air-quenching: (a) ^{11}B NMR spectrum of the air-quenched sample; (b) pore size distribution of the air-quenched sample after leaching.

3.2. Dependence of NMR Spectra on the Pore Size Distribution of Spinodal Phase Separation. Figures 6 and 7 show the ^{11}B NMR spectra and the corresponding domain size of phase separation for the sodium borosilicate glasses, which were prepared with varying quench rates. Samples exhibit a difference in pore size distribution with varying quench rates. The domain size of the phase separation for the sample by roller quenching (10^6 K/s) is around 0.35 nm. For the sample by air quenching (10 K/s), the domain size of the phase separation increases to ~0.45 nm. However, despite the variation of the domain size of the phase separation with cooling rate, the ^{11}B NMR spectra of the samples by both roller-quenching (10^6 K/s) and air-quenching (10 K/s) are almost exactly the same. The quantitative calculation shows that the fraction of four-coordinated boron is 29.08% in both the air-quenched sample and roller-quenched sample.

4. Discussion

4.1. Oxygen Diffusion Mechanism for Phase Separation. According to the investigation on the spinodal decomposition kinetics by Cahn,[15−17] the spinodal decomposition fluctuations at early stages are expressed as

$$A(\beta,t) = A(\beta,0)\exp[R(\beta)t] \quad (1)$$

where the amplification factor $R(\beta)$ is given by

$$R(\beta) = -(M\beta^2/N_v)[(f'' + 2k\beta^2] \quad (2)$$

Here $A(\beta,t)$ is the amplitude of a fluctuation of wavenumber β at time t; $A(\beta,0)$ is its initial amplitude, f'' is the second derivation of the free energy, $f(c)$, with respect to composition C, k is a constant, N_v is the number of molecules per unit volume, and M is the mobility, which is a function of the self-diffusion coefficients of individual elements, such as O, Si, B, and Na for sodium borosilicate glasses. Tomozawa has precisely measured the mobility M in the spinodal phase-separated glasses by X-ray small angle scattering,[19] which showed the order of magnitude of the mobility M is approximately equal to that of oxygen. This indicates that the spinodal phase separation is controlled by the slowest moving species, which is most likely oxygen. The rate controlling character of oxygen in phase separation has also been indicated by Weyl and Marboe.[48]

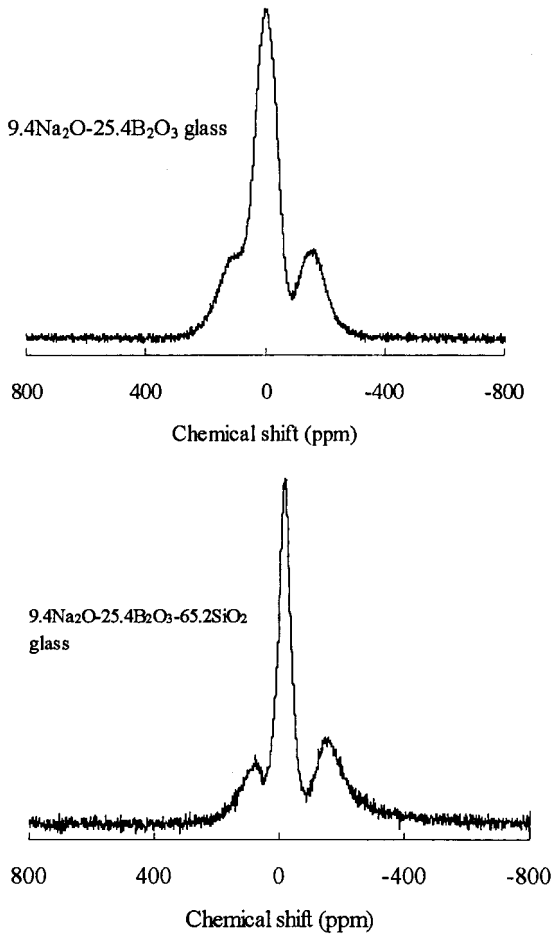

Figure 8. ^{11}B NMR spectra of $9.4Na_2O$-$25.4B_2O_3$-$65.2SiO_2$ ternary glass and $9.4Na_2O$-$25.4B_2O_3$ binary glass.

The mechanism of the oxygen diffusion of glasses in the alkali silicate system was investigated by many researchers.[49−51] It is usually thought that the controlling diffusion step in silicate glasses is the rupture of a single nonbridged oxygen bond to silicon. The diffusion mechanism is the interstitial motion of the ruptured nonbridging oxygen through voids in the lattice. By the interstitial model, it is not necessary to rupture two bands to silicon in order to free the oxygen ion, and subsequently, this kind of interstitial motion does not use up much energy and is therefore very probable.[51,52] It is assumed that the interstitial model is dominant when there exist lots of single nonbridged oxygen bonded to silicon.

However, this investigation shows that most of the oxygen in the sodium borosilicate glass exists as bridged ones, which leads to difficulty in explaining the oxygen diffusion process by the interstitial model. Figure 8 exhibits the ^{11}B NMR spectrum of $9.4Na_2O-25.4B_2O_3-65.2SiO_2$ ternary glass and $9.4Na_2O-25.4B_2O_3$ binary glass. The results of a quantitative calculation of the spectra for the $9.4Na_2O-25.4B_2O_3-65.2SiO_2$ ternary glass and $9.4Na_2O-25.4B_2O_3$ binary glass are shown in Figure 9. For $9.4Na_2O-25.4B_2O_3$ binary glass, the N_4 is

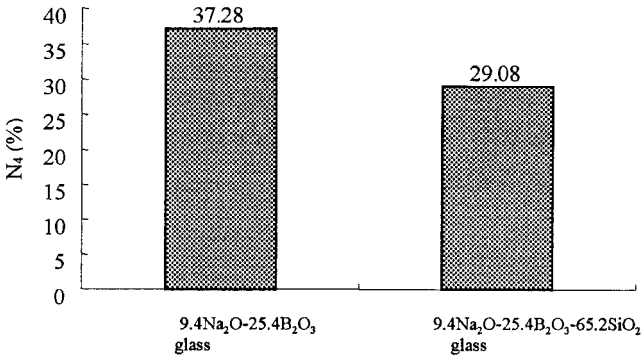

Figure 9. Comparison of the fraction of the four-coordinated boron (N_4) between $9.4Na_2O-25.4B_2O_3$ glass and $9.4Na_2O-25.4B_2O_3-65.2SiO_2$ glass.

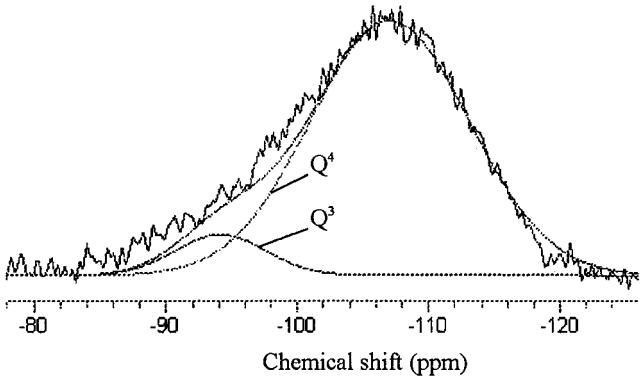

Figure 10. ^{29}Si NMR spectrum of the $Na_2O-B_2O_3-SiO_2$ glasses.

exactly equal to the mole ratio of sodium oxide to boron oxide, which indicates the sodium oxide associates itself with the boron network and is employed entirely to convert BO_3 units to BO_4 units.[35] Although a slight decrease of N_4 in $9.4Na_2O-25.4B_2O_3-65.2SiO_2$ glass can be observed, most of the BO_4 units, which is about 80% of the BO_4 units in the $9.4Na_2O-25.4B_2O_3$ binary glass, are still kept in $9.4Na_2O-25.4B_2O_3-65.2SiO_2$ glass, as shown in Figure 9. This suggests that, in $9.4Na_2O-25.4B_2O_3-65.2SiO_2$ glass, only a small amount of the sodium oxide associates itself with the silicon network. According to Figure 9, the distribution of the sodium oxide among the boron network and the silicon network in $9.4Na_2O-25.4B_2O_3-65.2SiO_2$ glass can be expressed as

$$9.4Na_2O-25.4B_2O_3-5.2SiO_2 \rightarrow (7.3Na_2O-5.4B_2O_3)-(2.1Na_2O-5.2SiO_2)$$

The nonbridged oxygens in silicate glass are formed through the sodium oxide associated with silicon network by the following reaction model:

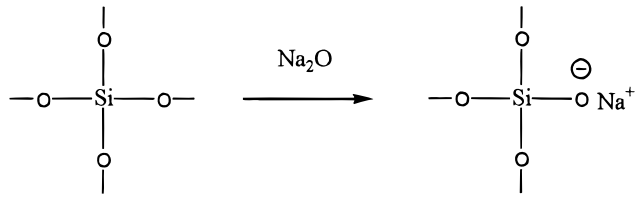

Considering that there is only small amount of the sodium oxide associated with the silicon network, it is assumed that most of silicate groups are SiO_4 tetrahedra connected by bridged oxygen.

Figure 10 shows the ^{29}Si MAS NMR spectra of the $Na_2O-B_2O_3-Si_2O$ glasses. ^{29}Si MAS NMR is capable of discriminating by characteristic chemical shifts between the five different SiO_4 tetrahedra connected with 0−4 other such tetrahedra, i.e., Q^0, Q^1, Q^2, Q^3, and Q^4 (the superscript gives the number, *m*, of SiOSi linkages of the $Si(OSi)_m(O-)_{4-m}$ structural units Q^m). The usual values for the mean chemical shifts used to fit the spectra of glasses are −107 ppm (Q^4), −92 ppm (Q^3), −82 ppm (Q^2), −69 ppm (Q^1), and −63 ppm (Q^0).[53] It is apparent that, by Figure 10, the spectrum mainly results from the Q^4 tetrahedra, which is completely connected with bridged oxygen. The relative proportions of Q^4 tetrahedra and Q^3 tetrahedra can be quantified by calculating the spectral area from Q^4 and Q^3. The calculation results of the ^{29}Si spectra (Figure 10) show that there is about 95% Q^4 against total Si network. The ^{29}Si spectra coincide well with the ^{11}B NMR measurement results. Thus, we think the vacancy motion, which is extensively discussed in section 4.2, rather than the interstitial motion of the oxygen resulting from the rupture of a single nonbridged oxygen bond to silicon, becomes the controlling factor in the diffusion step in the sodium borosilicate glasses.

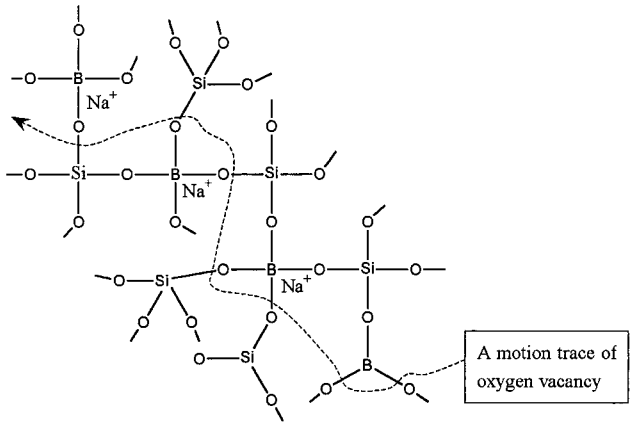

Figure 11. Illustration suggesting a motion trace of oxygen vacancy among neighboring-bridged oxygens in sodium borosilicate glass.

4.2. Structural Change on Rapid Quenching by the Mechanism of Oxygen Vacancy Motion. Since there exists few single nonbridged oxygens bonded to silicon in the sodium borosilicate glass, the vacancy motion of oxygen, rather than the interstitial motion of the oxygen, is expected to cause oxygen diffusion. The oxygen diffusion by the vacancy motion results in spinodal phase separation on quenching.

It is well-known that, at temperatures above absolute zero, the atoms of a solid execute vibrational motion about equilibrium positions. On the basis of the fact that phase separation occurs on quenching (Figures 4 and 5), it is assumed that the oxygen atom will have a large enough oscillation to break away from its equilibrium position during quenching of the sodium borosilicate glass through a spinodal region. Thus, some fraction of lattice oxygen atoms in local area will be breaking away from their tetrahedra to form vacancies in the lattice of the local area. The vacancies are positions around the silica tetrahedra or BO_3/BO_4 group where an oxygen ion should be. Although there is no change in the ^{11}B NMR spectra at varying quenching rate, as shown in Figures 6a and 7a, the variation of the domain size of the spinodal phase separation with quenching rate indeed occurs, as shown in Figures 4, 5, 6b, and 7b and Table 1. The unchanged ^{11}B NMR spectra at varying quenching rate itself suggests that the spinodal phase separation propagates without the change of the coordination number of boron. The model that may coincide with the above facts is that oxygen vacancies diffuse through the sodium borosilicate glass by rotating and

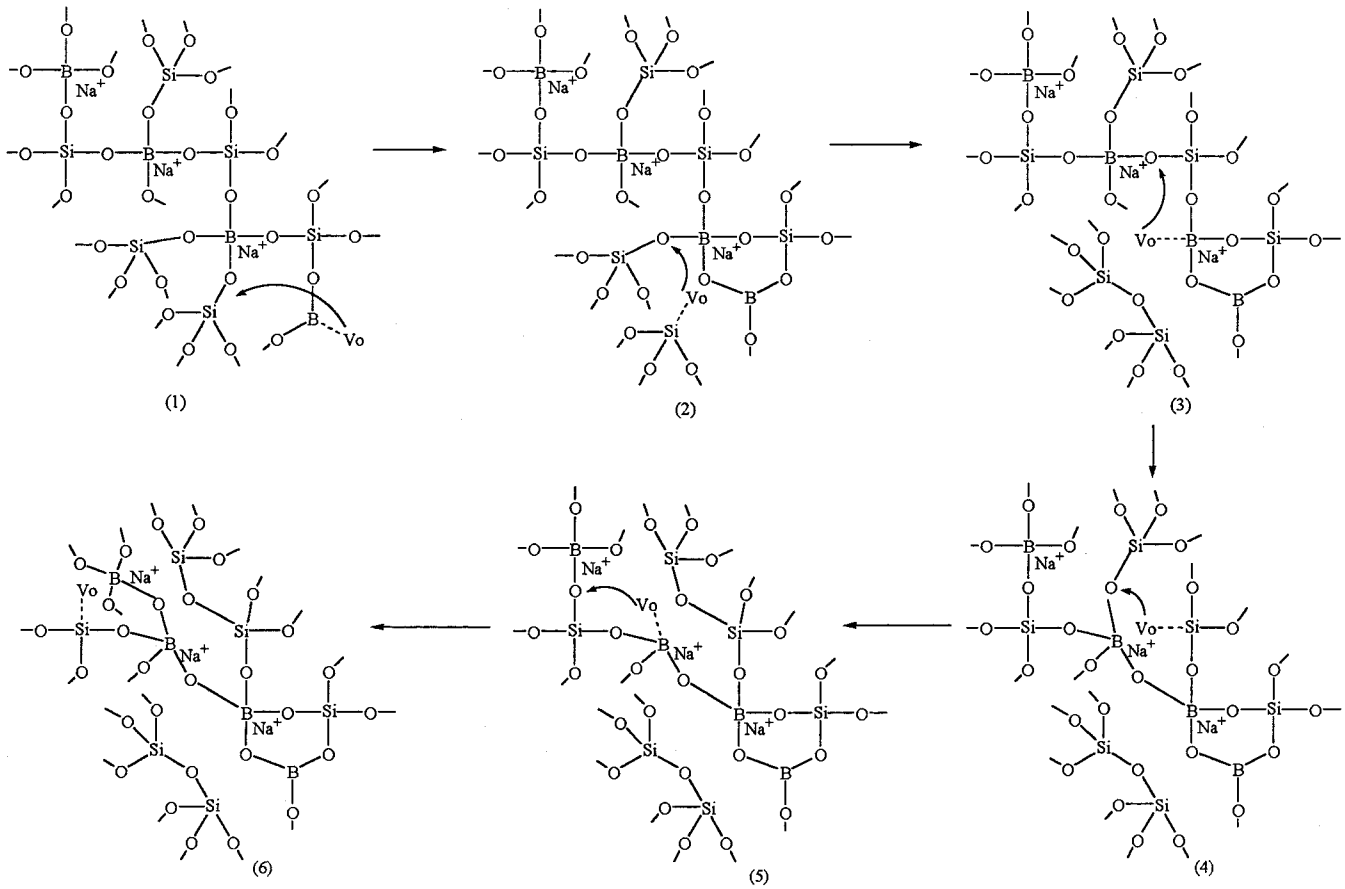

Figure 12. Illustration showing structural change by oxygen vacancy motion, which results in spinodal phase separation.

reacting with neighbor-bridged oxygen by the following mechanism where Vo is an oxygen vacancy. By means of such a

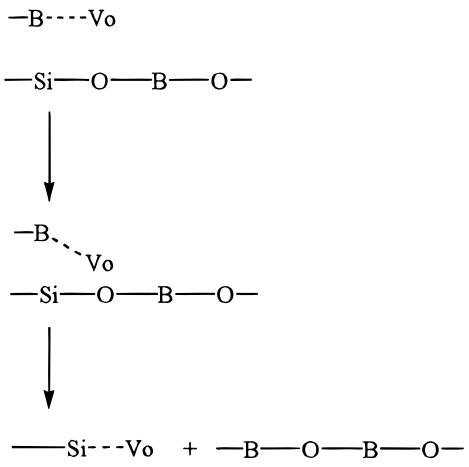

reaction the boron groups gradually change their neighbor from a silicon group to boron groups while the coordination number of boron is not changed. Consequently, a boron-rich phase with high connectivity can be formed along the motion trace of the oxygen vacancy.

Let us consider the two-dimensional representation of an ideal homogeneous sodium borosilicate glass with a vacancy of oxygen moving among neighboring bridged oxygen during quenching through the spinodal region, as shown in Figure 11. According to the rotation and reaction model of the oxygen vacancy mentioned above, the oxygen vacancy transfers among B−O bonds and neighboring Si−O bonds. Therefore, the boron units connect each other step by step, as shown in Figure 12, finally resulting in the formation of a boron-rich chain along the vacancy motion trace. By such a model, it is easy to image that the boron-rich chain can further grow by the diffusion of oxygen vacancies, which move along or across the chain. One BO_4 /BO_3 group has a size of 0.3−0.4 nm in diameter. Since the present experimental result shows the domain size is 0.7 nm in diameter for the spinodal phase separation on the roller-quenched process (Figure 6), the cross section of the boron-rich chain formed under roller-quenched process is composed of double BO_4/BO_3 groups.

One of the important characteristics of the spinodal phase separation based on the model of oxygen vacancy motion is the independence of the coordination number of the borate network and silicate network on the domain size of the spinodal phase separation, as shown in Figure 12. This coincides well with the measurement results of ^{11}B NMR spectra, which show no variation with the increase of the domain size of the phase separation (Figures 6 and 7). This investigation also checked the ^{29}Si MAS NMR spectra of samples that were prepared with varying quench rates. As shown in Figure 13, the results exhibited unchanged ^{29}Si MAS NMR spectra with quenching rate. The measurement result of the ^{29}Si MAS NMR spectra further supports the proposed mechanism of oxygen vacancy motion for spinodal phase separation in the sodium borosilicate glass.

By Figure 6b, it can be seen that when the quenching rate decreases, the domain size of the spinodal phase separation increases from 0.7 to 0.9 nm. The experimental results suggest that the cross section of the boron-rich chain increases from double BO_4/BO_3 groups to larger BO_4/BO_3 groups. Figure 14 shows the Raman spectra of the sodium borosilicate glasses that were prepared with varying quench rates. There is a slight

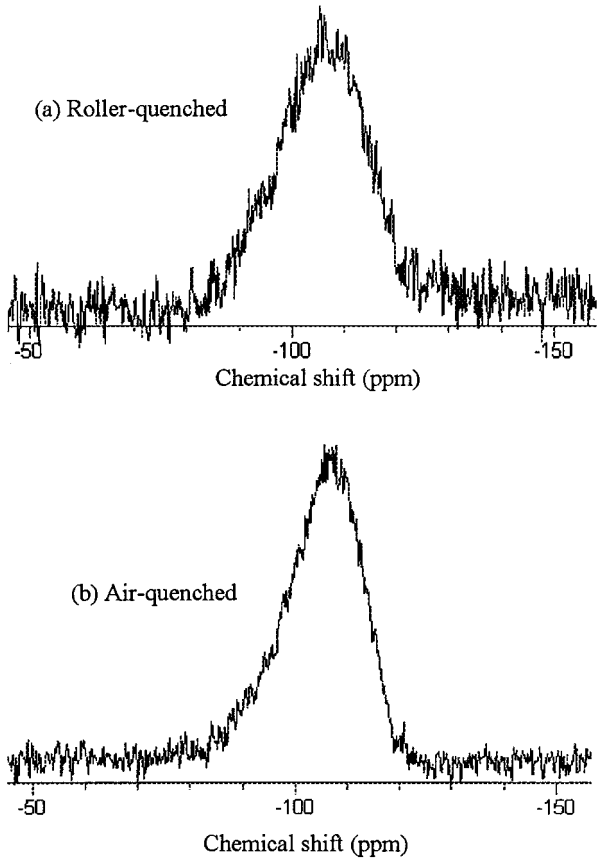

Figure 13. ^{29}Si MAS NMR spectra of the samples prepared with varying quench rates.

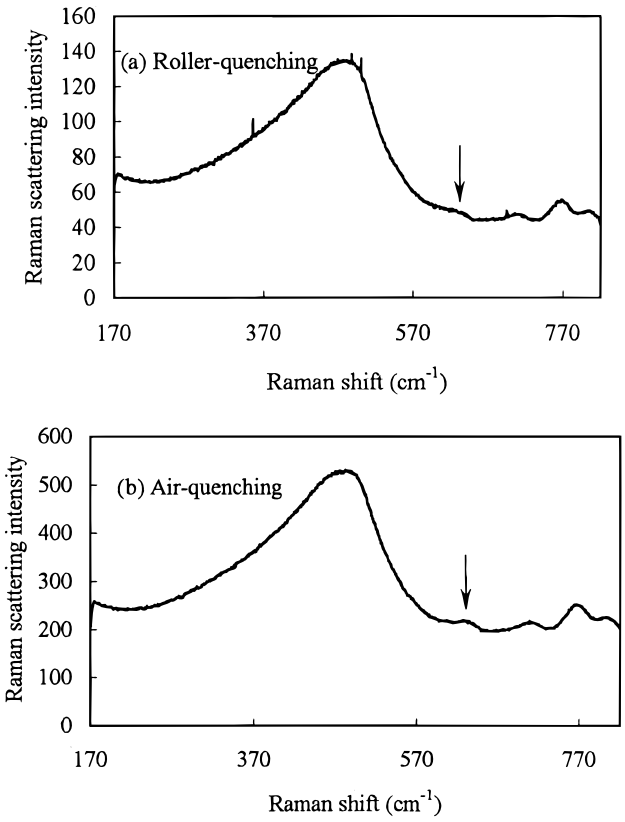

Figure 14. Raman spectra of the samples prepared with varying quench rates.

change for the band at about 630 cm^{-1}. White[54,55] has suggested that the band at 630 cm^{-1} for sodium borosilicate glasses may be due to the borate group. Therefore, the change at 630 cm^{-1} is caused by the formation of some new borate groups in the air-quenched sample. According to the measurement of pore size distribution (Figure 6b), it is mostly possible that the new borate group is the triborate group with the size of ~1 nm, as following illustrated. The change from double BO_4/BO_3 groups

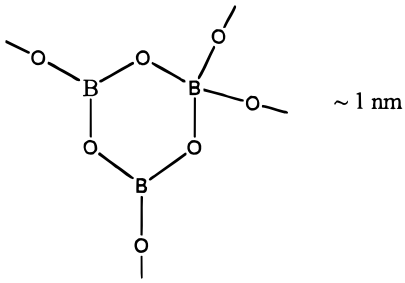

to triborate groups for the cross section of the boron-rich chain results in the growth of the boron-rich chain and subsequently the increase in the domain size of the phase separation.

5. Conclusions

1. For the $9.4Na_2O-25.4B_2O_3-65.2SiO_2$ (mol %) glass, boron atoms and most of the silicon atoms connect to bridged oxygen to form a network. Thus, the vacancy motion of the oxygen rather than the interstitial motion of the oxygen becomes the controlling step for the spinodal phase separation in the initial stage.

2. The oxygen vacancy may migrate through the sodium borosilicate glass by rotating to neighboring-bridged oxygen and reacting with neighboring-bridged oxygen. By means of such a reaction, the boron groups gradually change their neighbor from a silicon group to boron groups, resulting in the spinodal phase separation in the initial stage.

3. On rapid quenching, the spinodal phase separation has already occurred in the sodium borosilicate glasses by the formation of a boron-rich chain according to the oxygen vacancy motion model. The cross section of the boron-rich chains are composed of double boron groups or triborate groups.

4. One of the important characteristics of the spinodal phase separation based on the model of oxygen vacancy motion is the independence of the coordination number of the borate network and silicate network on the domain size of the spinodal phase separation. The experimental results showed that ^{11}B NMR spectra and ^{29}Si MAS NMR spectra did not change with the increase of the domain size of the phase separation. The experimental data supported the proposed mechanism of oxygen vacancy motion for spinodal phase separation in the sodium borosilicate glass.

References and Notes

(1) Yazawa, T. *Key Eng. Mater.* **1996**, *15*, 125.
(2) Kokubu, T.; Yamane, M. *J. Mater. Sci.* **1985**, *20*, 4309.
(3) Maekawa, H.; Maekawa, T.; Kawamura, K.; Yokokawa, T. *J. Non-Cryst. Solids* **1991**, *127*, 53.
(4) Yazawa, T.; Tanaka, H.; Eguchi, K.; Yokoyama, S. *J. Mater. Sci.* **1994**, *29*, 3433.
(5) Tanaka, H.; Yazawa, T.; Eguchi, K.; et al. *J. Non-Cryst. Solids* **1984**, *65*, 301.
(6) Yazawa, T.; Tanaka, H.; Eguchi, K.; Yokoyama, S.; Arai, T. *J. Mater. Sci. Lett.* **1993**, *12*, 263.
(7) Yazawa, T.; Tanaka, H.; Eguchi, K. *J. Mater. Sci. Lett.* **1993**, *13*, 494.
(8) Yazawa, T.; Miyake, A.; Tanaka, H. *J. Ceram. Soc. Jpn.* **1991**, *99*, 1094.
(9) Yazawa, T.; Tanaka, H.; Nakamichi, H.; et al. *J. Ceram. Soc. Jpn.* **1991**, *99*, 1271.

(10) Yazawa, T.; Tanaka, H.; Nakamichi, H.; Eguchi, K. *J. Ceram. Soc. Jpn*. **1988**, *96*, 630.
(11) Yazawa, T.; Tanaka, H.; Nakamichi, H.; Eguchi, K. *J. Ceram. Soc. Jpn*. **1988**, *96*, 18.
(12) Kuraoka, K.; Tanaka, H.; Yazawa, T. *J. Mater. Sci. Lett.* **1996**, *15*, 1.
(13) Kuraoka, K.; Qun, Z.; Kushibe, K.; Yazawa, T. *Sep. Sci. Technol.* **1998**, *33*, 297.
(14) Cahn, J. W.; Hilliard, J. E. *J. Chem. Phys.* **1959**, *31*, 688.
(15) Cahn, J. W. *J. Chem. Phys.* **1965**, *42*, 93.
(16) Cahn, J. W.; Charles, R. J. *Phys. Chem. Glasses* **1965**, *6*, 181.
(17) Tomozawa, M.; MacCrone, R. K.; Herman, H. *Phys. Chem. Glasses* **1970**, *11*, 136.
(18) Hammel, J. J. *J. Chem. Phys.* **1967**, *46*, 2234.
(19) Haller, W. *J. Chem. Phys.* **1965**, *42*, 686.
(20) Burnett, D. G.; Douglas, R. W. *Phys. Chem. Glasses* **1970**, *11*, 125.
(21) Mazurin, O. V.; Porai-Koshifts, E. A. *Phase separation in glass*; North-Holland: Amsterdam, 1984; Chapter 2, p 16.
(22) Yun, Y. H.; Bray, P. J. *J. Noncryst. Solids* **1978**, *27*, 363.
(23) Gresch, R.; Muller-Warmuth, W.; Dutz, H. *J. Noncryst. Solids* **1976**, *21*, 31.
(24) Milberg, M. E.; O'Keefe, J. G.; Verhelst, R. A.; Hooper, H. O. *Phys. Chem. Glasses* **1972**, *13*, 79.
(25) Beekenkamp, P. *Phys. Chem. Glasses* **1968**, *9*, 14.
(26) Bishop, S. G.; Bray, P. J. *Phys. Chem. Glasses* **1966**, *7*, 73.
(27) Rhee, C.; Bray, P. J. *Phys. Chem. Glasses* **1971**, *12*, 165.
(28) Park, M. J.; Bray, P. J. *Phys. Chem. Glasses* **1972**, *13*, 50.
(29) Kim, K. S.; Bray, P. J. *J. Nonmetal*. **1974**, *2*, 95.
(30) Kim, K. S.; Bray, P. J. *Phys. Chem. Glasses* **1974**, *15*, 47.
(31) Kim, K. S.; Bray, P. J. Merrin, S. *J. Chem. Phys.* **1976**, *64*, 4459.
(32) Chen, H. S.; Miller, C. E. *Rev. Sci. Instrum.* **1970**, *41*, 1237.
(33) Fenzke, D.; Freude, D.; Frolich, T.; Hasse, J. *Chem. Phys. Lett.* **1984**, *111*, 171.
(34) Kriz, H. M.; Park, M. J.; Bray, P. J. *Phys. Chem. Glasses* **1971**, *12*, 45.
(35) Du, W. F.; Kuraoka, K.; Akai, T.; Yazawa, T. *J. Ceram. Soc. Jpn.* **1999**, *107*, 1151.
(36) Brunauer, S.; Emmett, P. H.; Teller, E. *J. Am. Chem. Soc.* **1938**, *60*, 309.
(37) Mikhail, R. S.; Brunauer, S.; Bodor, E. E. *J. Colloid Interface Sci.* **1968**, *26*, 45.
(38) IUPAC Manual of Symbols and Terminology, Appendix 2. *Pure Appl. Chem*. **1972**, *31*, 578.
(39) Yazawa, T.; Tanaka, H.; Nakamichi, H.; Eguchi, K. *J. Ceram. Soc. Jpn*. **1987**, *95*, 1186.
(40) Dollimore, D.; Shingles, T. *J. Appl. Chem.* **1969**, *19*, 218.
(41) Avery, R. G.; Ramsay, J. D. F. *J. Colloid Interface Sci*. **1973**, *42*, 597.
(42) Shull, C. G. *J. Am. Chem. Soc.* **1948**, *70*, 1410.
(43) Dullien, F. A. L.; Dhawan, G. K. *J. Colloid Interface Sci*. **1974**, *47*, 337.
(44) Liabastre, A. A.; Orr, C. *J. Colloid Interface Sci*. **1978**, *64*, 1.
(45) Lecloux, A.; Pirard, J. P. *J. Colloid Interface Sci*. **1979**, *70*, 265.
(46) Putnam, F. A.; Fort, T. *J. Phys. Chem.* **1975**, *79*, 459.
(47) Gregg, S. J.; Sing, K. S. W. *Adsorption, Surface Area and Porosity*; Academic Press Inc., New York, 1982.
(48) Weyl, W. A.; Marboe, E. C. *The constitution of glasses*; Interscience Publishers: New York and London, 1964; Vol. 2, Part 1, p 712.
(49) Kingery, W. D.; Lecron, J. A. *Phys. Chem. Glasses* **1960**, *1*, 87.
(50) Williams, E. L. *J. Am. Ceram. Soc.* **1965**, 48, 190−194.
(51) Terai, R.; Hayami, R. *J. Noncryst. Solids* **1975**, *18*, 217.
(52) Sucov, E. W. *J. Am. Ceram. Soc.* **1963**, *46*, 14.
(53) Lippmaa, E.; Magi, M.; Samoson, A.; et al. *J. Am. Chem. Soc.* **1980**, *102*, 4889.
(54) Furukawa, T.; White, W. B. *J. Mater. Sci.* **1981**, *16*, 2689.
(55) White, W. B. *J. Noncryst. Solids* **1982**, *49*, 321.